

Influence of random pinning on melting scenario of two-dimensional core-softened potential system

E. N. Tsiok, Yu. D. Fomin, and V. N. Ryzhov¹

¹ *Institute for High Pressure Physics RAS, 108840 Kaluzhskoe shosse, 14, Troitsk, Moscow, Russia*
(Dated: August 19, 2016)

The random disorder can drastically change the melting scenario of two-dimensional systems and has to be taken into account in the interpretation of the experimental results. We present the results of the molecular dynamics simulations of the two dimensional system with the core-softened potentials with two repulsive steps in which a small fraction of the particles is pinned, inducing quenched disorder. It is shown that without the quenched disorder the system with small repulsive shoulder, which is close in the shape to the soft disks, melts in accordance with the melting scenario proposed in Refs. [30, 31, 33] (first-order liquid-hexatic and continuous hexatic-solid transitions). Random pinning widens the hexatic phase, but leaves the melting scenario unchanged. For the system with larger repulsive step at high densities the conventional first-order transition takes place without random pinning. However, in the presence of disorder the single first-order transition transforms into two transitions, one of them (solid-hexatic) is the continuous KTHNY-like transition, while the hexatic to isotropic liquid transition occurs as the first order transition.

PACS numbers: 61.20.Gy, 61.20.Ne, 64.60.Kw

INTRODUCTION

Nature of two-dimensional melting is one of the long-standing problems in condensed matter physics. Despite a lot of publications in past forty years, the controversy about the microscopic nature of melting in two dimensions (2D) still lasts. In contrast to the three dimensional case, where melting occurs through the conventional first order transition, several microscopic scenarios were proposed for the microscopic description of 2D melting. The reason of this difference is the drastic increase of fluctuations in 2D in comparison with the 3D case. Landau, Peierls and Mermin [1] showed that in two dimensions the long-ranged positional order can not exist because of the thermal fluctuations and transforms to the quasi-long-ranged one. On the other hand, the real long-ranged orientational order (the order in directions of the bonds joining the particle with its nearest neighbors) does exist in this case.

Now the Kosterlitz-Thouless-Halperin-Nelson-Young (KTHNY) theory of 2D melting [2–5] is the most widely accepted. In this theory it was proposed that 2D solids melt through two continuous transitions, which are induced by the formation of the topological defects. For example, an elementary topological defect of the triangular lattice is a disclination. Disclination in a triangular crystal lattice is defined as an isolated defect with five or seven nearest neighbours. A dislocation can be considered as a bound pair of 5 and 7-fold disclinations. In the framework of the KTHNY scenario, the 2D solid melts through dissociation of bound dislocation pairs. In this case the long-ranged orientational order transforms into quasi-long-ranged one, and quasi-long-ranged positional order becomes short-ranged. This new intermediate phase is called a hexatic phase. In turn, the hexatic

phase transforms into an isotropic liquid phase with a short-ranged orientational and positional orders through unbinding of dislocations (5 and 7-fold bound pairs) into free disclinations. It should be noted, that the KTHNY theory gives only limits of stability of the solid and hexatic phases and does not reject the possibility of the preempting first order liquid-solid transition with another melting mechanism.

The KTHNY theory seems universal and applicable to all system. However, it contains two phenomenological parameters, the core energy of dislocation E_c and Frank module of hexatic phase K_A , which do not have explicit expressions in terms of the interparticle potential. As it was shown later, with decreasing E_c melting can occur through a single first-order transition as a result of, for example, the formation of grain boundaries [18] or "explosion" of 5-7-5-7 quartets (bound dislocation pairs) into free disclinations [19].

Recently the KTHNY scenario was unambiguously experimentally confirmed for superparamagnetic colloidal particles interacting via long-range dipolar interaction [6–10]. In these experiments the particles are absorbed at liquid-air interface, which restricts the out-of-plane motion. On the other hand, in very popular experimental systems of colloidal particles confined between two glass plates [11] the melting transition consistent with the KTHNY scenario was found [12–14]. At the same time, a first order liquid-solid [15] and even a first-order liquid-hexatic and a first-order hexatic-solid phase transitions [16] are also possible. One can conclude from these results that the melting mechanism is not universal and depends on the interparticle interactions. However, controversies still exist even for the same systems, like, for example, for hard spheres [20–29].

Recently, another melting scenario was proposed [30–

35]. In contrast to the KTHNY theory, it was argued that in the basic hard disk model the hexatic phase does exist, and the system melts through a continuous solid-hexatic transition but a first-order hexatic-liquid transition [30–32]. In Ref. [34] it was shown that there is a first-order transition between the stable hexatic phase and isotropic liquid in $2D$ Yukawa system. In their work [33] Kapfer and Krauth have considered the behavior of soft disk system with the potential of the form $U(r) = (\sigma/r)^n$. They have shown that the system melts in accordance with the KTHNY theory for $n \leq 6$, while for $n > 6$ the two-stage melting transition takes place with the continuous solid-hexatic transition and the first-order hexatic-liquid one. Experimental confirmation of this scenario was found in the system of colloidal particles on water-decane interface [17]. It should be also noted the recent publication [36], where for the Herzian disks model it was shown that at low densities there is a discontinuous liquid-hexatic transition while at higher densities the system melts through the continuous Kosterlitz-Thouless transition.

In real experiments, two-dimensional confinement is typically realized in slit pores of different nature or by adsorption on solid substrates. In both cases the frozen-in (quenched) disorder due to some roughness or intrinsic defects can appear. Quenched disorder can change the melting scenario in $2D$. A disordered substrate can have the similar destructive effect on the crystalline order as temperature and can lead to the melting even at zero temperature [37–40]. In Refs. [37, 38] it was shown, that the KTHNY melting scenario persists in the presence of weak disorder. As it is intuitively clear, the temperature of the hexatic-isotropic liquid transition T_i is almost unaffected by disorder, while the melting temperature T_m drastically decreases with increasing disorder [37–40]. As a result, the stability range of the hexatic phase widens. These predictions have been confirmed in experiment and simulations of the system of superparamagnetic colloidal particles [9, 10]. In these experiments the particles form a monolayer on the bottom of a cylindrical glass cell of $5 - mm$ diameter due to gravity. Quenched disorder occurs due to pinning of a small amount of particles to the glass substrate due to van der Waals interactions and chemical reactions. In our simulations we tried to choose the simulation method in qualitative accordance with this experimental setup.

In this paper, we present a detailed computer simulation study of $2D$ phase diagram of the previously introduced core softened potential system [41–46] in the presence of the quenched disorder for different values of the width of the repulsive shoulder. Various forms of the core-softened potentials are widely used for the qualitative description of the water-like anomalous behavior, including density, structural and diffusion anomalies, liquid-liquid phase transitions, glass transitions, melting maxima [41–59]. In our previous publications the

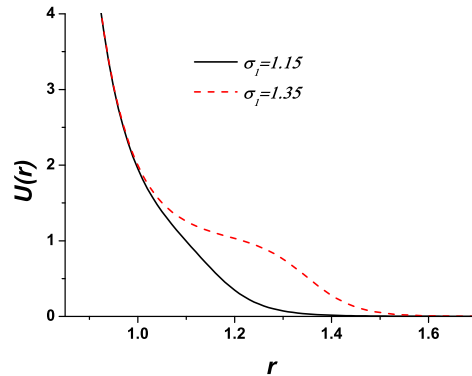


FIG. 1: The potential (1) with two different soft-core diameters: $\sigma_1/\sigma = 1.15; 1.35$.

preliminary result on the phase diagram of the system were reported [60–63]. It was shown that the random pinning widens the range of the hexatic phase and transforms the first-order melting at high densities into two transitions - first-order liquid-hexatic and continuous Kosterlitz-Thouless-like solid-hexatic transitions [64]. Here we present the corrected version of the phase diagram for the system with the larger repulsive shoulder, obtained with the use of additional criteria including the calculation of the diffusion coefficient of the hexatic phase.

We also study the system with small repulsive shoulder. It is shown, that in this case the behavior of the system is similar to the soft disks one [33]. The presence of the random pinning leads to drastic increase of the width of the hexatic phase, but does not change the melting scenario.

SYSTEMS AND METHODS

In the present simulations we study the system which is described by the potential [41–46, 60–62, 64]:

$$U(r) = \varepsilon \left(\frac{\sigma}{r} \right)^n + \frac{1}{2} \varepsilon (1 - \tanh(k_1 \{r - \sigma_1\})). \quad (1)$$

where $n = 14$ and $k_1 \sigma = 10.0$. σ is the hard-core diameter. We simulate the systems with two different soft-core diameters: $\sigma_1/\sigma = 1.15; 1.35$. (see Fig. 1).

In the remainder of this paper we use the dimensionless quantities, which in $2D$ have the form: $\tilde{\mathbf{r}} \equiv \mathbf{r}/\sigma$, $\tilde{P} \equiv P\sigma^2/\varepsilon$, $\tilde{V} \equiv V/N\sigma^2 \equiv 1/\tilde{\rho}$, $\tilde{T} \equiv k_B T/\varepsilon$, $\tilde{\sigma} = \sigma_1/\sigma$. In the rest of the article the tildes will be omitted.

In this article we make the molecular dynamics simulations in NVT and NVE ensembles in the framework of the LAMMPS package [66] with the number of particles from 20000 to 100000. In order to obtain the quenched

disorder in the system, we randomly choose a subset of particles at the random positions and let them to be immobile for the entire simulation run [64]. The simulations of 10 independent replicas of the system with different distributions of random pinned patterns were made. The thermodynamic functions were calculated by averaging over replicas. We calculate the pressure P versus density ρ along the isotherms, and the correlation functions $G_6(r)$ and $G_T(r)$ of the bond orientational ψ_6 and translational ψ_T order parameters (OPs), which characterize the overall orientational and translational order [64].

The translational ψ_T (TOP) and the orientational order parameters ψ_6 (OOP) along with the bond-orientational $G_6(r)$ (OCF) and translational $G_T(r)$ (TCF) correlation functions are defined in the conventional way [3, 4, 26, 28, 29, 36, 58, 59] with the subsequent averaging over the quenched disorder [64].

In accordance with the standard definitions [3, 4, 36], TOP has the form:

$$\psi_T = \frac{1}{N} \left\langle \left\langle \left| \sum_i e^{i\mathbf{G}\mathbf{r}_i} \right| \right\rangle \right\rangle_{rp}, \quad (2)$$

where \mathbf{r}_i is the position vector of particle i and \mathbf{G} is the reciprocal-lattice vector of the first shell of the crystal lattice. The translational correlation function can be obtained from the equation:

$$G_T(r) = \left\langle \frac{\langle \exp(i\mathbf{G}(\mathbf{r}_i - \mathbf{r}_j)) \rangle}{g(r)} \right\rangle_{rp}, \quad (3)$$

where $r = |\mathbf{r}_i - \mathbf{r}_j|$ and $g(r) = \langle \delta(\mathbf{r}_i) \delta(\mathbf{r}_j) \rangle$ is the pair distribution function. The second angular brackets $\langle \dots \rangle_{rp}$ correspond to the averaging over the random pinning. In the solid phase without random pinning the long range behavior of $G_T(r)$ has the form $G_T(r) \propto r^{-\eta_T}$ with $\eta_T \leq \frac{1}{3}$ [3, 4].

To measure the orientational order and the hexatic phase, the local order parameter which determines the 6-fold orientational ordering can be defined in the following way:

$$\Psi_6(\mathbf{r}_i) = \frac{1}{n(i)} \sum_{j=1}^{n(i)} e^{in\theta_{ij}}, \quad (4)$$

where θ_{ij} is the angle of the vector between particles i and j with respect to a reference axis and the sum over j is counting $n(i)$ nearest-neighbors of j , obtained from the Voronoi construction. The global OOP can be calculated as an average over all particles and random pinning:

$$\psi_6 = \frac{1}{N} \left\langle \left\langle \left| \sum_i \Psi_6(\mathbf{r}_i) \right| \right\rangle \right\rangle_{rp}. \quad (5)$$

The orientational correlation function $G_6(r)$ (OCF) is given in the similar way as in Eq. (3):

$$G_6(r) = \left\langle \frac{\langle \Psi_6(\mathbf{r}) \Psi_6^*(\mathbf{0}) \rangle}{g(r)} \right\rangle_{rp}, \quad (6)$$

where $\Psi_6(\mathbf{r})$ is the local bond-orientational order parameter (4). In the hexatic phase there is a quasi-long range order with the algebraic decay of the orientational correlation function $G_6(r) \propto r^{-\eta_6}$ with $0 \leq \eta_6 \leq \frac{1}{4}$ [3–5]. The stability criterion of the hexatic phase has the form $\eta_6(T_i) = \frac{1}{4}$.

The influence of disorder on the orientational and translational correlation functions has been considered in our previous publication [64] (see Fig. 1 in [64]). In the presence of pinning, it was not found any qualitative change in the behavior of $G_6(r)$ in accordance with the results of Nelson and coworkers [37, 38] and our intuitive expectations. On the other hand, the translational correlation function $G_T(r)$ demonstrates the qualitatively different behavior when the random disorder presents. Without pinning one has the conventional power law decay of TCF. In the case of pinning, the slope of the enveloping line increases at some crossover value r_0 . The region $r < r_0$ corresponds to the local order unaffected by quenched disorder, while asymptotic behavior of TCF for $r > r_0$ is determined by the random pinning [64]. It was also shown that, in accordance with the intuitive physical picture, r_0 decreases with increase of impurities concentration along with the increase of the slope of the enveloping line. The equality $\eta_T(T_m) = 1/3$ for the long range asymptote of TCF (for $r > r_0$) can be considered as the solid-hexatic stability criterion. The hexatic-liquid stability point corresponds to $\eta_6(T_i) = 1/4$ [37, 38].

RESULTS AND DISCUSSION

$$\sigma = 1.15$$

Let us first consider the behavior of the system with the small repulsive shoulder $\sigma = 1.15$. In this case, as one can see in Fig. 1, the form of the potential is very close to the soft disk with $n = 14$. The preliminary discussion of the phase diagram of this system can be found in Ref. [61], where the isotherms with the van der Waals loops are presented along with the phase diagram calculated with the help of the double-tangent construction to the Helmholtz free energy curves [65].

In Fig. 2 we show the orientational correlation functions (OCF) for the system without quenched disorder (a) and with the random pinning (concentration of pinning centers is 0.1%) at temperature $T = 0.2$. One can see that the behavior of the OCFs is equivalent for both cases, as it was discussed in the Introduction, and the limits of stability of the hexatic phase, determined from the condition $\eta = 1/3$, coincide too. From Fig. 2 it follows that the density at which hexatic phase becomes unstable is $\rho \approx 0.613$.

On the other hand, the translational correlation functions of the systems with and without random pinning are qualitatively different (see Fig. 3). In this case the

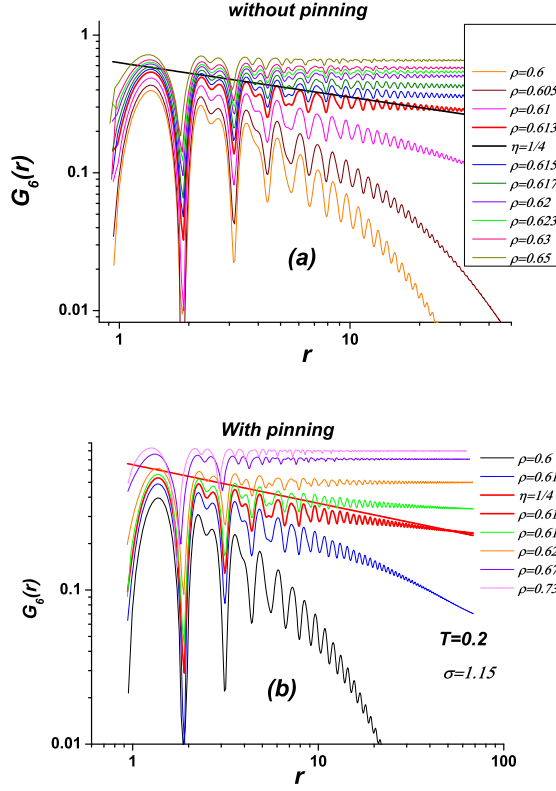


FIG. 2: OCF for different densities at $T = 0.2$ without random pinning (a) and concentration of the pinning centers 0.1% (b).

densities corresponding to the loss of stability of the solid phase are considerably different. From Fig. 3 (a) one can see that without pinning the stability limit corresponds to $\rho \approx 0.63$ while in the system with the quenched disorder the solid-hexatic stability limit is $\rho \approx 0.65$ (see Fig. 3 (b)).

In Fig. 4 the equation of state at $T = 0.2$ is presented. It is seen that the liquid-hexatic stability limit is located inside the Van der Waals loop region for both systems - with and without the random pinning. At the same time, for the pinning-free system the hexatic-solid stability limit is located outside the Van der Waals loop. One can conclude that in this case the system melts in accordance with the melting scenario proposed in Refs. [30, 31, 34].

In the presence of the random pinning the hexatic-solid instability density shifts to the higher densities, however, the melting scenario does not change. We have first-order liquid-hexatic transition and continuous hexatic-solid transition. In Fig. 5 the corresponding behavior of the orientational ψ_6 and translational ψ_T order parameters is shown. The orientational order parameter ψ_6 demonstrates the conventional behavior characteristic, for example, for the system without random pinning

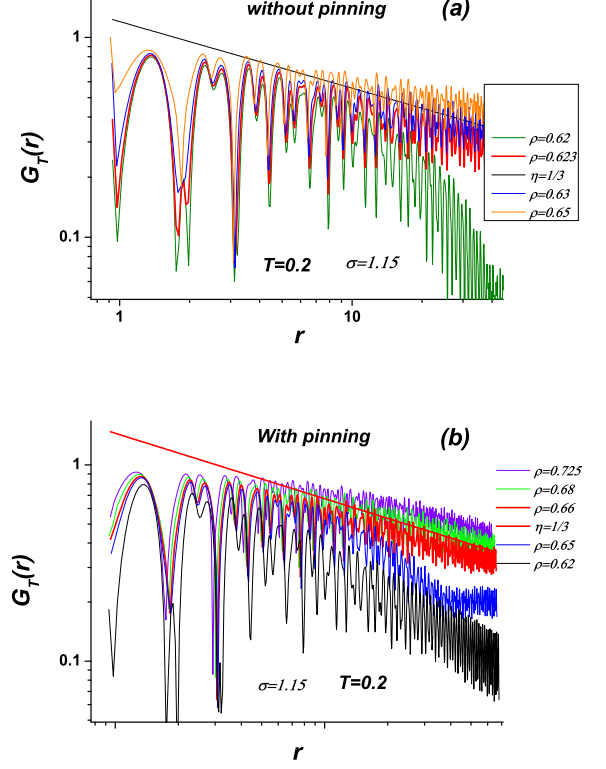


FIG. 3: TCF for different densities at $T = 0.2$ without random pinning (a) and concentration of the pinning centers 0.1% (b).

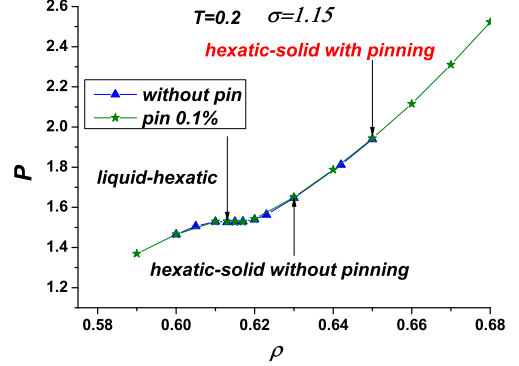


FIG. 4: Isotherms of the system with $\sigma = 1.15$ without pinning (triangles) and with the concentration of the pinning centers equal to 0.1% (stars) for $T = 0.2$.

[61]. However, the translational order parameter ψ_T has the qualitatively different form. In Fig. 5 one can see that the ψ_T curve has step-like behavior. In decreasing the density, ψ_T jumps downward at $\rho \approx 0.65$ corresponding to the stability limit of the solid phase in the presence of random pinning. On the other hand, ψ_T is not equal

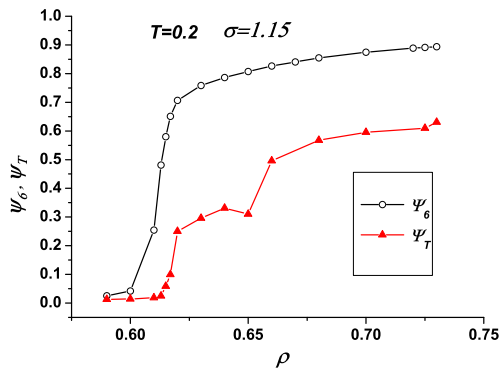


FIG. 5: The orientational Ψ_6 and translational Ψ_T order parameters for the system with random pinning and $\sigma = 1.15$.

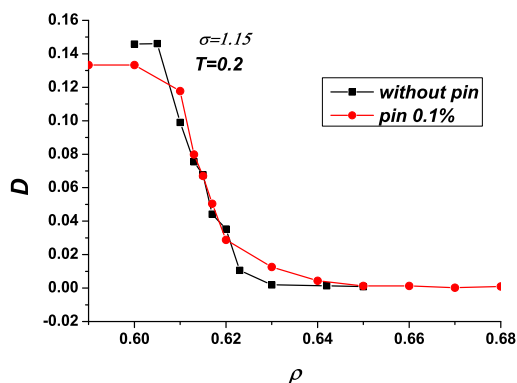


FIG. 6: The diffusion coefficient of the system with $\sigma = 1.15$ with (red circles) and without (black squares) random pinning.

to zero at $\rho \approx 0.65$ because the local translational order does exist in this state (see Fig. 3 and discussion in the previous Section). The translational order parameter disappears only in the two-phase region.

Because the translational order parameter ψ_T is not equal to zero in the hexatic phase, it is interesting to calculate the coefficient of diffusion in order to be sure that the system is really a liquid (but with quasi-long range orientational order). It should be noted that in the cases when the hexatic phase was reported (see, for example, [30, 31, 34, 59]) its density range is extremely narrow, and it is very difficult to calculate its dynamic properties. In the presence of quenched disorder the hexatic phase considerably widens, and the calculation of diffusion coefficient becomes more reliable. In Fig. 6 we present the diffusion coefficient for $\sigma = 1.15$ with and without random pinning. One can see that without pinning the increase of the diffusion coefficient begins at $\rho \approx 0.63$, while in

the system with random pinning the diffusion coefficient begins to become nonzero at $\rho \approx 0.65$ in accordance with the results shown in Figs. 4 and 5.

$$\sigma = 1.35$$

In the case of $\sigma = 1.35$, the results are more complex and interesting in comparison with the previous Subsection. As it was shown in our publications [60–64], the phase diagram of the system obtained with the help of the Helmholtz free energy calculations for different phases and construction of a common tangent to them [65] has three different crystal phases, one of them has square symmetry and the other two are the low density and high density triangular lattices (see, for example, Fig. 6 (a) in [62]). As it was suggested in [60–63], melting of the low density triangular phase is a continuous two-stage transition, with a narrow intermediate hexatic phase. This conclusion was made from the double-tangent construction and calculations of the behavior of OOPs and TOPs. However, the more precise analysis based on the study of the orientational and translational correlation functions is necessary. At the same time at high densities the square and triangular phases melt through the first order transitions. At high temperatures and high density there is one first order transition between triangular solid and isotropic liquid. It should be noted that the water-like thermodynamic and dynamic anomalies do exist in this case [62].

Let us first consider the effect of pinning on the high density part of the phase diagram where melting occurs through the first-order phase transition. Before to proceed, let us consider the behavior of the system without quenched disorder in more detail.

Fig. 7 illustrates the behavior of OCF and TCF for different densities at $T = 0.3$ without pinning ((a) and (b)) and with the concentration of the pinning centers equal to 0.1% ((c) and (d)). Using equations $\eta_T = 1/3$ and $\eta_6 = 1/4$, we calculated the limits of stability of hexatic and solid phases. One can see that without quenched disorder both these limits lie inside the two-phase region (Van der Waals loop) of the corresponding equation of state (see Fig. 8). From these results it is possible to conclude that in this case there is the only first-order liquid-solid transition without hexatic phase.

On the other hand, from Fig. 7 (c) one can see that random pinning leaves almost unaffected the limit of stability of the hexatic phase, while considerably changes the location of hexatic-solid transition (see Fig. 7 (d)). In this case the melting scenario qualitatively changes - instead of one first-order transition we have two-stage melting with first-order liquid-hexatic transition and continuous Kosterlitz-Thouless hexatic-solid transition with the intermediate hexatic phase. For the first time this kind of behavior was found in [64].

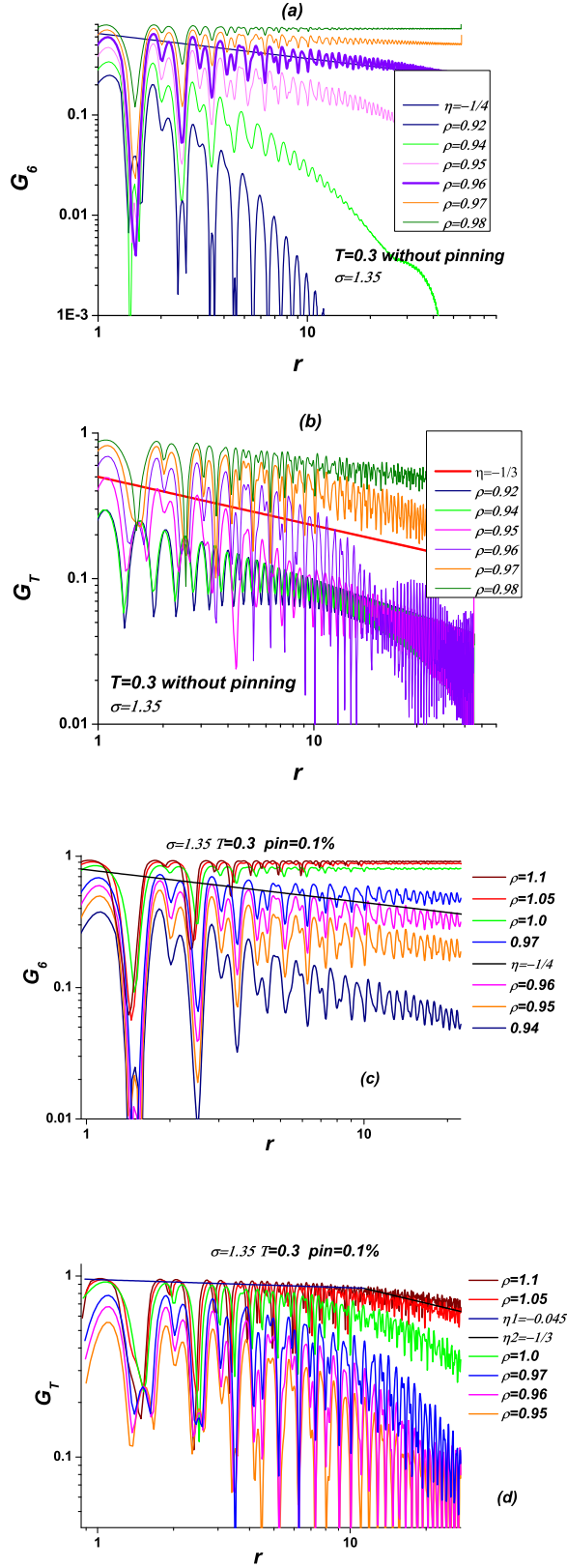


FIG. 7: OCF G_6 and TCF G_T for different densities at $T = 0.3$ without random pinning ((a) and (b)) and concentration of the pinning centers 0.1% ((c) and (d)) for $\sigma = 1.35$.

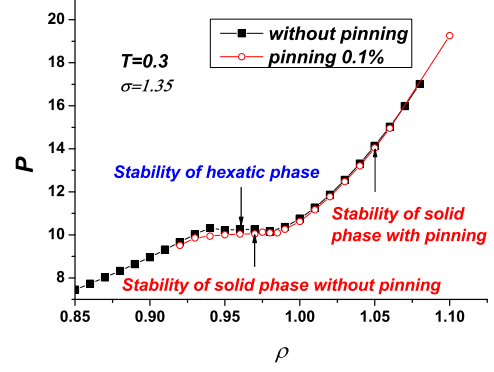


FIG. 8: Isotherms of the system with $\sigma = 1.35$ without pinning (squares) and with the concentration of the pinning centers equal to 0.1% (empty circles) for $T = 0.3$.

Even more interesting picture takes place at low densities. In Fig. 9 we present the OCFs and TCFs for the system without random pinning at $T = 0.12$ at densities corresponding to the left and right borders of the "cupola" of the triangular solid at low density part of the phase diagram (see Fig. 6 (a) in [62] and Fig. 12). In Fig. 10 the isotherms corresponding to these borders are shown for the same temperature $T = 0.12$. One can see, that the limits of stability determined from the equations $\eta_T = 1/3$ for the solid phase and $\eta_6 = 1/4$ for the hexatic phase are inside the two-phase region of the first-order melting transition of the system without pinning for the left part of the dome, while at the right border of the dome the line of solid-hexatic transition obtained from condition $\eta_T = 1/3$ is outside of the two-phase region (see Fig. 10). From this picture one can conclude that without random pinning at the low density border of the dome the system melts through one first-order transition, while at high density (right) border the two-stage melting takes place with first-order liquid-hexatic transition and continuous hexatic-solid one.

As it was discussed above, random pinning leaves almost unaffected the line of the liquid-hexatic transition, while considerably changes the location of hexatic-solid stability limit. At the same time, the Van der Waals loops which are characteristic of the first order transition are almost unchanged by impurities. As a result, in the presence of random pinning the hexatic phase drastically widens in accordance with the theoretical predictions [9, 10, 37, 38, 64], while in the case of the single first-order melting the transitions splits into first-order liquid-hexatic transition and continuous hexatic-solid transition. The stability limits of the hexatic-solid transitions at $T = 0.12$ in the presence of the random pinning are shown in Fig. 10.

As in the previous subsection, we calculated the diffusion coefficient of the system without and with random

pinning (Fig. 11) for $\rho = 0.48$. One can see that without pinning the increase of the diffusion coefficient begins at $T \approx 0.18$, while in the system with random pinning the diffusion coefficient begins to become nonzero at $T \approx 0.15$ in accordance with the results shown in Fig. 12 (b).

The results characterizing the influence of random pinning on the phase diagram of the system with $\sigma = 1.35$ are shown in Fig. 12. The effect of random pinning on the first-order melting transition is shown in Fig. 12 (a) for the temperatures higher than 0.3. It should be noted that the phase diagram was calculated using the double-tangent construction to the Helmholtz free energy and the Maxwell construction for the corresponding Van der Waals loops. In this case, as it was discussed above, the transition in the pure system is of first order. The line where $G_6(r)$ decays algebraically with the exponent equal to $1/4$ is located inside the two-phase region. At the same time, in the presence of random pinning the line of solid-hexatic transition obtained from condition $\eta_T = 1/3$ is shifted to higher densities, and random pinning transforms the single first-order transition into two transition with rather wide hexatic phase. The solid-hexatic transition is continuous, while the hexatic phase transforms into isotropic liquid through first-order transition.

In Fig. 12 (b) we plot the low-density part of the phase diagram. The dashed lines correspond to the two-phase regions obtained with the help of the Maxwell constructions for the corresponding Van der Waals loops. One can see that without random pinning the limits of stability of the hexatic phase obtained from the equation $\eta_6 = 1/4$ are inside the two-phase region for both the left and right borders of the dome, while the hexatic-solid transition lines calculated from the equation $\eta_T = 1/3$ have different locations: it is inside the two-phase region for the left border and outside for the right one. As it was discussed above, in the left part of the phase diagram the system melts through a single first-order transition, however, at the left part melting occurs through two transitions with the narrow intermediate hexatic phase and first-order liquid-hexatic transition and continuous hexatic-solid one. In the presence of quenched disorder the hexatic phase appears at the left part of the phase diagram and considerably widens at the right part.

CONCLUSIONS

In conclusion, in this paper we present the computer simulation study of melting transition of 2D core soft-ened system with two lengths of the repulsive shoulder (Eq. (1) and Fig. 1) in the presence of random pinning. It is shown that without the quenched disorder the system with small repulsive shoulder $\sigma = 1.15$ which is close in the shape to the soft disks $1/r^n$ with $n = 14$ melts in accordance with the melting scenario proposed in Refs. [30, 31, 33] (first-order liquid-hexatic and contin-

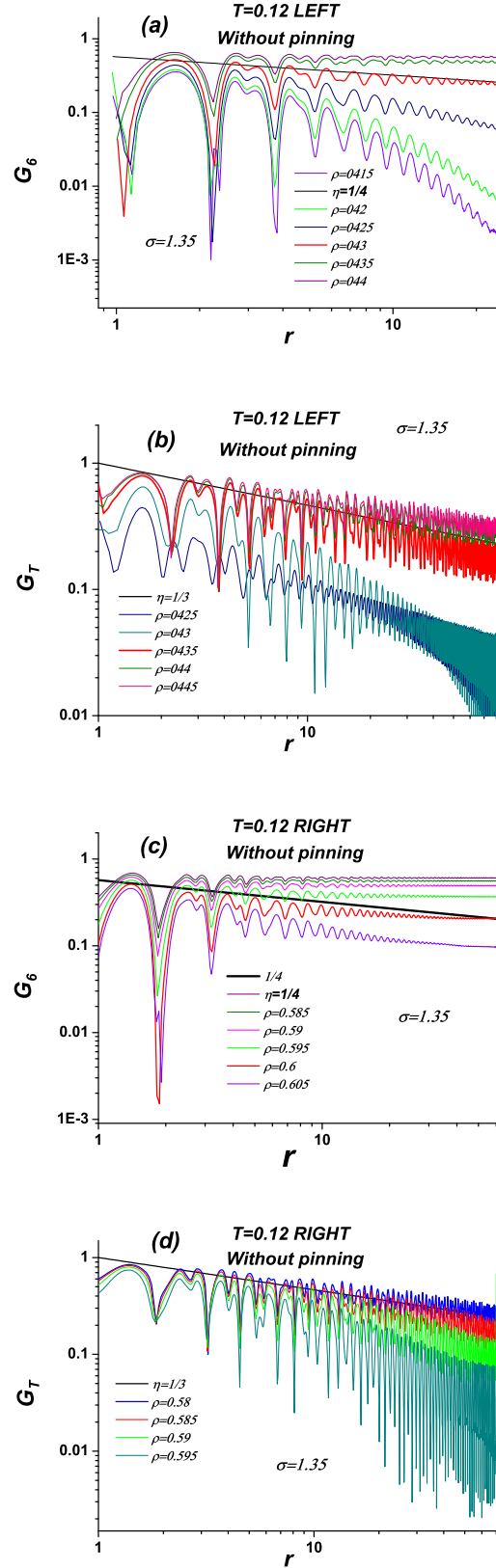


FIG. 9: OCF G_6 and TCF G_T for different densities at $T = 0.12$ without random pinning for left ((a) and (b)) and right ((c) and (d)) branches of dome at the low-density part of the phase diagram (see, for example, Fig. 6 (a) in [62]) for $\sigma = 1.35$.

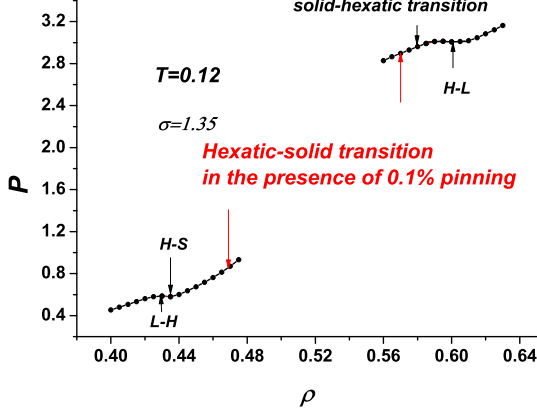


FIG. 10: Isotherms of the system with $\sigma = 1.35$ without random pinning and with the concentration of the pinning centers equal to 0.1% for $T = 0.12$.

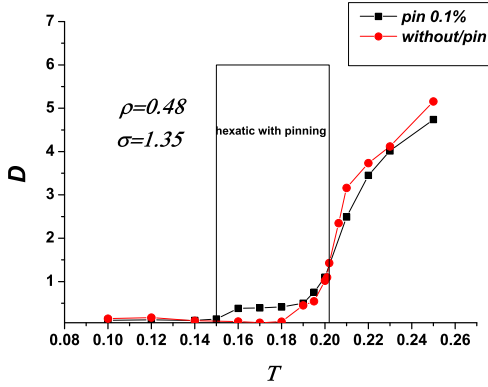


FIG. 11: The diffusion coefficient of the system with $\sigma = 1.35$ with (red circles) and without (black squares) random pinning.

uous hexatic-solid transitions). Random pinning widens the hexatic phase, but leaves the melting scenario unchanged.

Melting of the system with larger repulsive step $\sigma = 1.35$ is much more complex (see Fig. 12). At high densities the conventional first-order transition takes place without random pinning (Fig. 12 (a)). However, disorder drastically changes this melting scenario. The single first-order transition transforms into two transitions, one of them (solid-hexatic) is the continuous KTHNY-like transition, while the hexatic to isotropic liquid transition occurs as the first order transition in accordance with the recently proposed scenarios [30, 31, 33]. The possible mechanism for this transition is the spontaneous proliferation of grain boundaries [18, 32, 34]. This scenario of melting in the presence of pinning was proposed in Ref. [64]. It should be noted, that melting scenario with the single first-order transition corresponds to the system at

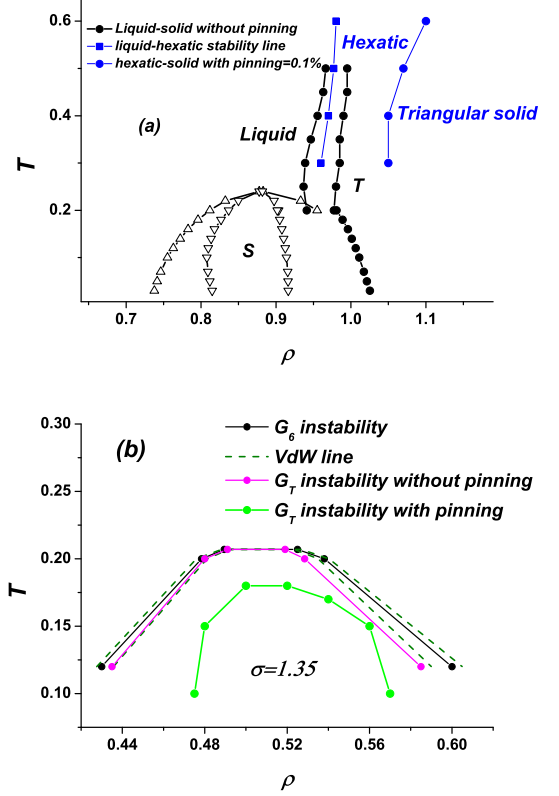


FIG. 12: Phase diagram of the system with $\sigma = 1.35$: (a) high density part with first order solid-liquid transition without random pinning (black lines) and two transitions - first-order liquid-hexatic and continuous hexatic-solid - for the concentration of the pinning centers equal to 0.1%; (b) low-density part of the phase diagram. Dashed lines corresponds to the first order transition calculated from Maxwell construction for the Van der Waals loops (see Fig. 10). Without random pinning melting occurs through the first-order transition on the left branch of the dome, while at right branch melting scenario corresponds to two transitions - first-order liquid-hexatic and continuous hexatic-solid. Green line demonstrates the shift of the hexatic-solid transition in the presence of the random pinning.

low enough temperature. At high temperatures the repulsive shoulder of the potential becomes ineffective, and the properties of the potential will be similar to the soft disks $1/r^n$ with $n = 14$. In this case one can expect that there is critical temperature (some kind of tricritical point) above which melting should occur through two transitions in accordance with the scenario proposed in Ref. [33].

At low densities the system without pinning melts through the single first-order transition at the left border of the dome (Fig. 12) (b), while at the right border one can observe the two-stage melting in accordance with the scenario proposed in [30, 31, 33]. The similar behavior was recently found in the system of Herizian disks [36].

The random pinning transforms the first-order transition at left border into two transitions with wide hexatic phase and widens the hexatic phase at the right border.

It should be noted, that the nature of the first-order liquid-hexatic transition is still puzzling, because the conventional theory like the KTHNY one can not describe the first-order liquid-hexatic transition.

The results of this study can be useful for the qualitative understanding the behavior of water confined in the hydrophobic slit nanopores [67], especially because the square solid structure was found (see Fig. 12) that is similar to the one discovered in experiment [67].

The authors are grateful to S.M. Stishov and V.V. Brazhkin for valuable discussions. We thank the Russian Scientific Center at Kurchatov Institute and Joint Supercomputing Center of Russian Academy of Science for computational facilities. The work was supported by the Russian Science Foundation (Grant No 14-12-00820).

-
- [1] N. D. Mermin, Phys. Rev. **176**, 250 (1968).
 - [2] M. Kosterlitz and D.J. Thouless, J. Phys. C **6** 1181 (1973).
 - [3] B.I. Halperin and D.R.Nelson, Phys. Rev. Lett. **41** 121 (1978).
 - [4] D.R.Nelson and B.I. Halperin, Phys. Rev. B **19** 2457 (1979).
 - [5] A.P. Young, Phys. Rev. B **19** 1855 (1979).
 - [6] Urs Gasser, C. Eisenmann, G. Maret, and P. Keim, ChemPhysChem **11**, 963 (2010).
 - [7] K. Zahn and G. Maret, Phys. Rev. Lett. **85** 3656 (2000).
 - [8] P. Keim, G. Maret, and H.H. von Grunberg, Phys. Rev. E **75**, 031402 (2007).
 - [9] S. Deutschlander, T. Horn, H. Lowen, G. Maret, and P. Keim, Phys. Rev. Lett. **111**, 098301 (2013).
 - [10] T. Horn, S. Deutschlander, H. Lowen, G. Maret, and P. Keim, Phys. Rev. E **88**, 062305 (2013).
 - [11] S. A. Rice, Chem. Phys. Lett., 2009, **479**, 1.
 - [12] C. A. Murray and D. H. Van Winkle, Phys. Rev. Lett., 1987, **58**, 1200.
 - [13] R. E. Kusner, J. A. Mann, J. Kerins and A. J. Dahm, Phys. Rev. Lett., 1994, **73**, 3113.
 - [14] Y. Han, N. Y. Ha, A. M. Alsayed and A. G. Yodh, Phys. Rev. E, 2008, **77**, 041406.
 - [15] P. Karnchanaphanurach, B. Lin and S. A. Rice, Phys. Rev. E, 2000, **61**, 4036.
 - [16] A. H. Marcus and S. A. Rice, Phys. Rev. Lett., 1996, **77**, 2577; Phys. Rev. E, 1997, **55**, 637.
 - [17] B.-J. Lin and L.-J. Chen, J. Chem. Phys., 2007, **126**, 034706.
 - [18] S.T. Chui, Phys. Rev. B **28**, 178 (1983).
 - [19] V.N. Ryzhov, Zh. Eksp. Teor. Fiz. **100**, 1627 (1991) [Sov. Phys. JETP **73**, 899 (1991)].
 - [20] V.N. Ryzhov and E.E. Tareyeva, Phys. Rev. B **51** 8789 (1995).
 - [21] V.N. Ryzhov and E.E. Tareeva, Zh. Eksp. Teor. Fiz. **108**, 2044 (1995) [J. Exp. Theor. Phys. **81**, 1115 (1995)].
 - [22] V.N. Ryzhov and E.E. Tareyeva, Physica A **314**, 396 (2002).
 - [23] V.N. Ryzhov and E.E. Tareyeva, Theor. Math. Phys. **130**, 101 (2002) (DOI: 10.1023/A:1013884616321).
 - [24] P. Bladon and D. Frenkel, Phys. Rev. Lett. **74**, 2519 (1995).
 - [25] J. Lee and K.J. Strandburg, Phys. Rev. B **46**, 11190 (1992).
 - [26] H. Weber, D. Marx, and K. Binder, Phys. Rev. B **51**, 14636 (1995).
 - [27] C.H. Mak, Phys. Rev. E **73**, 065104 (2006).
 - [28] K. Binder, S. Sengupta, and P. Nielaba, J. Phys.: Condens. Matter **14**, 2323 (2002).
 - [29] K. Wierschem and E. Manousakis, Phys. Rev. B **83**, 214108 (2011).
 - [30] E.P. Bernard and W. Krauth, Phys. Rev. Lett. **107**, 155704 (2011).
 - [31] M. Engel, J.A. Anderson, S.C. Glotzer, M. Isobe, E.P. Bernard, W. Krauth, Phys. Rev. E **87**, 042134 (2013).
 - [32] W. Qi, A. P. Gantapara and M. Dijkstra, Soft Matter **10**, 5449 (2014).
 - [33] S.C. Kapfer and W. Krauth, Phys. Rev. Lett. **114**, 035702 (2015).
 - [34] W.K. Qi, S.M. Qin, X.Y. Zhao, and Yong Chen, J. Phys.: Condens. Matter **20**, 245102 (2008).
 - [35] W. Qi and M. Dijkstra, Soft Matter **11**, 2015, 2852 (DOI: 10.1039/c4sm02876g).
 - [36] M. Zu, J. Liu, H. Tong, and N. Xu, arXiv:1605.00747v1.
 - [37] D. R. Nelson, Phys. Rev. B **27**, 2902 (1983).
 - [38] S. Sachdev and D. R. Nelson, J. Phys. C-Solid State Physics **17**, 5473 (1984).
 - [39] Min-Chul Cha and H. A. Fertig, Phys. Rev. Lett. **74**, 4867 (1995).
 - [40] S. Herrera-Velarde and H. H. von Grunberg, Soft Matter, **5**, 391 (2009).
 - [41] Y.D. Fomin, N.V. Gribova, V.N. Ryzhov, S.M Stishov, and D. Frenkel, J. Chem. Phys. **129**, 064512 (2008).
 - [42] N.V. Gribova, Y.D. Fomin, D. Frenkel, and V.N. Ryzhov, Phys. Rev. E **79** 051202 (2009).
 - [43] Y.D. Fomin, E.N. Tsiok, and V.N. Ryzhov, J. Chem. Phys. **135**, 234502 (2011).
 - [44] Y.D. Fomin, E.N. Tsiok, and V.N. Ryzhov, J. Chem. Phys. **135**, 124512 (2011).
 - [45] R.E. Ryltsev, N.M. Chtchelkatchev, and V.N. Ryzhov, Phys. Rev. Lett. **110**, 025701 (2013).
 - [46] Y.D. Fomin, E.N. Tsiok, and V.N. Ryzhov, Phys. Rev. E **87**, 042122 (2013).
 - [47] S.V. Buldyrev, G. Malescio, C.A. Angell, N. Giovambattista, S. Prestipino, F. Saija, H.E. Stanley, and L. Xu, J. Phys.: Condens. Matter **21**, 504106 (2009).
 - [48] P. Vilaseca and G. Franzese, Journal of Non-Crystalline Solids **357**, 419 (2011).
 - [49] G. Franzese, J. Mol. Liq. **136**, 267 (2007);
 - [50] Pol Vilaseca and Giancarlo Franzese, J. Chem. Phys. **133**, 084507 (2010).
 - [51] F. Leonia and G. Franzese, J.Chem.Phys. **141**, 174501 (2014).
 - [52] A. B. de Oliveira, P. A. Netz, T. Colla, and M. C. Barbosa, J. Chem. Phys. **124**, 084505 (2006).
 - [53] L.B. Krott and M.C. Barbosa, J. Chem. Phys. **138** 084505 (2013).
 - [54] L. B. Krott and M. C. Barbosa, Phys. Rev. E **89**, 012110 (2014).
 - [55] L. B. Krott, J. R. Bordin, and M.C. Barbosa, J. Phys.

- Chem. B **119**, 291 (2015).
- [56] A.M. Almudallal, S.V. Buldyrev, and I. Saika-Voivod, J. Chem. Phys., **137** 034507 (2012).
 - [57] M.R. Sadr-Lahijany, A. Scala, S.V. Buldyrev, H.E. Stanley, Phys. Rev. Lett. **81**, 4895 (1998).
 - [58] S. Prestipino, F. Saija, and P.V. Giaquinta, J. Chem. Phys. **137**, 104503 (2012).
 - [59] S. Prestipino, F. Saija, and P.V. Giaquinta, Phys. Rev. Lett. **106**, 235701 (2011).
 - [60] D.E. Dudalov, Yu.D. Fomin, E.N. Tsiok, and V.N. Ryzhov, J. Phys.: Conference Series **510**, 012016 (2014) (doi:10.1088/1742-6596/510/1/012016).
 - [61] D.E. Dudalov, Yu.D. Fomin, E.N. Tsiok, and V.N. Ryzhov, J. Chem. Phys. **141**, 18C522 (2014).
 - [62] D.E. Dudalov, Yu.D. Fomin, E.N. Tsiok, and V.N. Ryzhov, Soft Matter **10**, 4966 (2014).
 - [63] E.S. Chumakov, Y.D. Fomin, E.L. Shangina, E.E. Tareyeva, E.N. Tsiok, V.N. Ryzhov, Physica A **432**, 279 (2015).
 - [64] E. N. Tsiok, D. E. Dudalov, Yu. D. Fomin, and V. N. Ryzhov, Phys. Rev. E **92**, 032110 (2015).
 - [65] Daan Frenkel and Berend Smit, *Understanding molecular simulation (From Algorithms to Applications)*, 2nd Edition (Academic Press, 2002).
 - [66] <http://lammps.sandia.gov/>
 - [67] G. Algara-Siller, O. Lehtinen, F. C. Wang, R. R. Nair, U. Kaiser, H. A.Wu, A. K. Geim, I. V. Grigorieva, Nature **519**, 443 (2015).